Journal of Nanostructure in Chemistry
a SpringerOpen Journal

ORIGINAL Open Access

Visible-light-activated nanocomposite photocatalyst of Cr_2O_3/SnO_2

Rajendra Bhosale[1], Sidram Pujari[1], Gajanan Muley[2], Bathuwell Pagare[3] and Anil Gambhire[3*]

Abstract

Visible-light-activated Cr_2O_3/SnO_2 nanocomposite photocatalyst was prepared by coprecipitation method and characterized by X-ray diffraction, transmission electron microscopy, X-ray photoelectron spectroscopy, N_2 adsorption-desorption measurement, and UV–vis diffuse reflectance spectroscopy. The results show that phase composition, crystallite size, Brunauer-Emmett-Teller surface area, and optical absorption of samples varied significantly with the heat treatment temperatures. The Cr_2O_3/SnO_2 photocatalyst (the molar ratio Cr to Sn is 1:2) calcined at 400°C for 2 h exhibited maximum photocatalytic activity because it has a smaller particle size of 10.05 nm and a higher surface area of 38.75 m^2/g. Under visible-light ($\lambda > 400$ nm) irradiation, the degradation rate of Rhodamine B reached 98.0% in 60 min, which is about 3.5 times higher than that of the standard P25 photocatalyst.

Keywords: Coprecipitation method, Coupled photocatalyst, Photocatalytic activity, Photoelectron spectroscopy

Background

In recent years, photocatalytic degradation of various kinds of organic–inorganic pollutants using semiconductor powder as a photocatalyst has been extensively studied [1,2]. Among various oxide semiconductor photocatalysts, TiO_2 was intensively investigated because of its biological and chemical inertness, strong oxidizing power, nontoxicity, and long-term stability [3-5]. However, the photocatalytic activity of TiO_2 (the bandgap is 3.2 eV, and it can be excited by photons with wavelengths below 387 nm) is limited to irradiation wavelengths in the UV region so that the effective utilization of solar energy is limited to about 3% to 5% of the total solar spectrum. Furthermore, the fast recombination of photo-generated electron–hole pairs hinders the commercialization of this technology [6]. The decomposition of adsorbed organic compound is closely correlated with the density of space charge-separated electron–hole pair on TiO_2. Therefore, it is of great interest to separate the electron–hole pairs effectively to increase the photon efficiencies and develop new visible-light photocatalyst to extend the absorption wavelength range into the visible-light region. In this sense, an interesting approach to deal with the issue is carried out by coupled semiconductor technique. Recently, there are a number of studies related to the photocatalytic activity of coupled semiconductor photocatalyst such as ZnO/SnO_2 [6], SnO_2-TiO_2 [7], Au/TiO_2-CeO_2 [8], and TiO_2-CdS [9]. The results show that nearly all the composite semiconductors have presented higher photocatalytic activity than single ones. Indeed, this effect could be due to the synergistic effect of the coupled semiconductor photocatalyst. It was also reported that the chromium-doped TiO_2 has been found to exhibit superior photocatalytic activity under visible-light irradiation because chromium atom can effectively narrow the energy bandgap of TiO_2 [10,11]. Chromium-based catalysts have been widely examined for polymerization, partial oxidation, and aromatization reaction because of the peculiar characteristics of Cr oxide species on the surface of the support, including oxidation state and coordination environment [12]. However, there have been few studies clearly elucidating the roles of the surface chromate species and supporting the oxidation reaction, particularly the decomposition of environmental pollutants.

In this study, a series of Cr_2O_3/SnO_2 photocatalysts with different calcination temperatures were prepared by coprecipitation method, and their phase compositions, crystalline structures, and particle sizes were studied. We also explored their photocatalytic degradation performance

* Correspondence: abg_chem@ymail.com
[3]Department of Chemistry, Shri Anand College of Science, Pathardi, Ahmednagar, Maharashtra 414102, India
Full list of author information is available at the end of the article

in treating Rhodamine B solution under visible-light (λ > 400 nm) irradiation.

Results and discussion

XRD analysis

Figure 1 shows X-ray diffraction (XRD) patterns of the Cr_2O_3/SnO_2 photocatalysts calcined at different temperatures for 2 h. It can be seen that the diffraction pattern of the sample prepared at 300°C is indistinct because of the amorphous configuration. While the sample calcined at 400°C, the diffraction peaks clearly show that the Cr_2O_3 and SnO_2 nanocrystals coexisted in the samples. With the increase of calcination temperature (at 500°C), the phase composition is still the mixture of Cr_2O_3 and SnO_2 phase, but the peak intensity of the sample obviously increases due to the growth of crystallites and enhancement of crystallization. Table 1 summarizes the

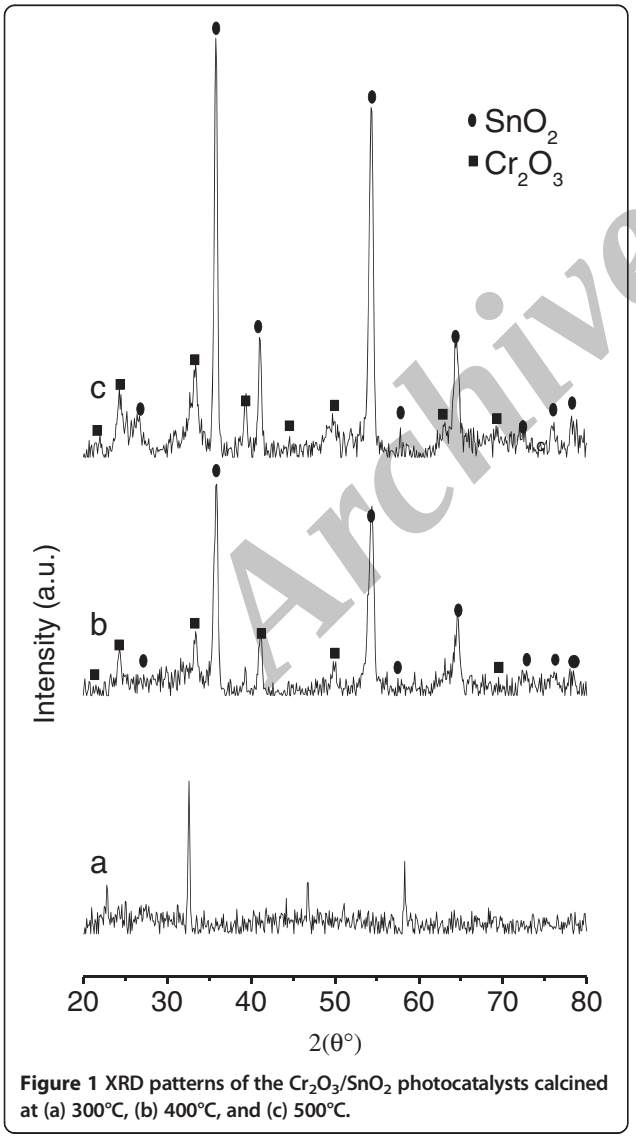

Figure 1 XRD patterns of the Cr_2O_3/SnO_2 photocatalysts calcined at (a) 300°C, (b) 400°C, and (c) 500°C.

Table 1 Effect of calcination temperature on average particle size and BET surface area of Cr_2O_3/SnO_2 samples

Calcination temperature (°C)	BET surface area (m^2/g)	Grain size (nm)
300	–	6.80
400	38.75	10.05
500	19.02	23.15
600	8.35	31.19

Brunauer-Emmett-Teller (BET) surface area and grain size of the samples. The average grain sizes estimated from the highest intensity diffraction peaks of SnO_2 (2θ = 33.37) using Scherrer's equation were 6.80, 10.05, and 23.15 nm for samples a, b, and c, respectively. It is obvious that the grain sizes of the samples improved with the increase of heat treatment temperature, while the BET surface areas decreased.

TEM analysis

The grain sizes of the Cr_2O_3/SnO_2 nanocomposite photocatalysts varied with calcination temperature, which has been confirmed in the transmission electron microscopy (TEM) images (Figure 2a,b,c,d). It can be seen that the sample calcined at 300°C appeared amorphous because of its weak crystallization, and the grain edge of the sample was a little dim. The TEM images also indicated that the grain size was homogenous and fairly small (about 10 nm) when the sample was calcined at 400°C. In contrast, the sample calcined at 500°C displayed greater particle size due to the enhancement of crystallization or sintering between smaller particles, which is estimated to be about 25 nm. The increase of heat treatment temperature caused the catalyst grains to become larger. The result was in agreement with that of XRD. Figure 2d shows a high-resolution (HR) TEM image of Cr_2O_3/SnO_2 powder calcined at 400°C and its corresponding fast Fourier transform (FFT) pattern. The space between adjacent lattice planes is 0.32 nm, corresponding to 110 planes of rutile SnO_2. Combined with the results of FFT analysis, the preferential growth direction is (112).

UV–vis DR spectral analysis

Figure 3 gives the UV–vis diffuse reflectance spectra (DRS) of the Cr_2O_3/SnO_2 photocatalysts calcined at 300°C, 400°C, and 500°C. A progressive red shift in the bandgap absorption is noticed with the increase of calcination temperature. This implies that the absorption edges of the samples shift to the longer wavelength range. When calcined at 300°C, the sample has a little absorption in the range of visible light (λ > 400 nm) because the catalyst is mainly composed of amorphous SnO_2 powder (shown in XRD patterns), which is only effective under ultraviolet irradiation. With the increase

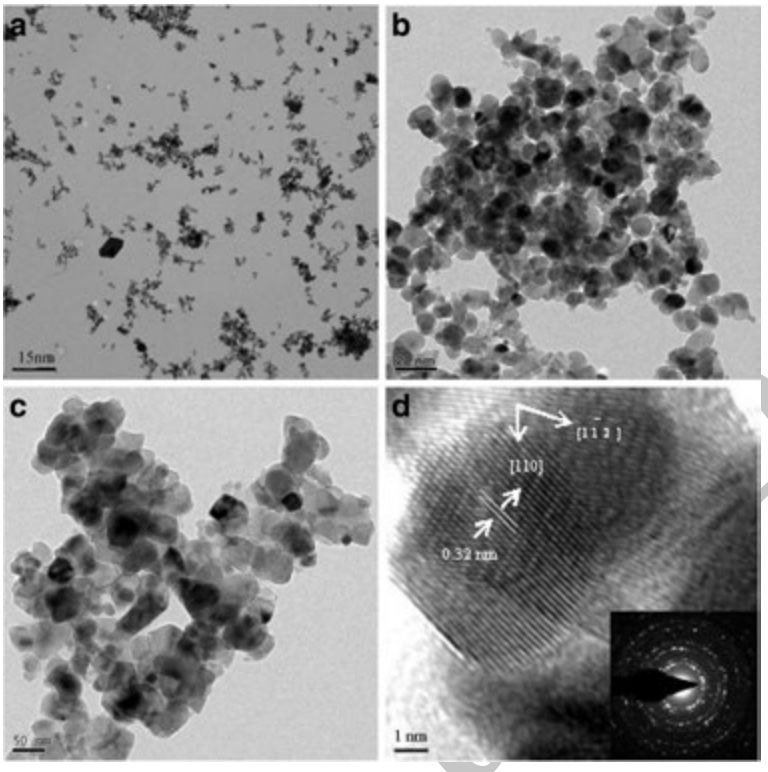

Figure 2 TEM images of Cr_2O_3/SnO_2 photocatalyst calcined at different temperatures, HRTEM image, and inset of FFT. TEM images at (**a**) 300°C, (**b**) 400°C, and (**c**) 500°C; (**d**) HRTEM image of photocatalyst (**b**); and inset of corresponding FFT of (**d**).

of calcination temperature (reaching 400°C), the absorption edge of the sample has some red shift. The red shift is presumably ascribed to the formation of the homogeneous Cr_2O_3 nanocrystals. The absorption onsets were determined by linear extrapolation from the infection point of the curve to the baseline. The edges of the absorption of the Cr_2O_3 incorporated SnO_2 samples were shifted to approximately 500 nm, corresponding to a bandgap energy of 2.25 eV.

The bandgap energy of Cr_2O_3 is 2.5 eV and can be activated by the light below 560 nm [13], when it couples with SnO_2 semiconductor, the conduction band of SnO_2 acts as a sink for photo-generated electrons. The photo-generated holes move in the opposite direction and accumulate in the valence band of the Cr_2O_3 particle, which leads to increasing the charge separation efficiency and extending the photo-responding range to visible light. When the heat treatment temperature reaches 500°C, the crystallite sizes become larger, and the absorption edge shows more red shift.

XPS studies

Figure 4a,b,c shows the high-resolution X-ray photoelectron spectroscopy (XPS) spectra of the $Cr2p_{3/2}$, O 1s, and Sn 3d regions, taken on the surface of Cr_2O_3/SnO_2 photocatalyst calcined at 400°C. The $Cr2p_{3/2}$ level (Figure 4a) is broad and showed asymmetry towards higher binding-energy side of the main peak. The deconvolution of the $Cr2p_{3/2}$ signals based upon the previous studies [14] and the comparison to the reference samples including CrO_3 and Cr_2O_3 indicate that spectra for the present catalytic systems contain two major peaks at 579.1 eV for Cr(VI) and 576.1 eV for Cr(III). The change in oxidation state of chromium from sixth to third might be due to oxide/oxide support interaction. From high-resolution XPS spectra of O 1s region (Figure 4b), it can be seen that oxygen on the sample surface exists at least in three forms: at the binding energy of 530.4 eV which corresponds to oxygen in SnO_2 lattice; 531.7 eV which corresponds to oxygen in SnO_2 surface adsorption of (–OH); and 533.5 eV which corresponds to oxygen in SnO_2 surface adsorption of H_2O. It is just because so much adsorption oxygen exists on the SnO_2 surface that they become captives of photo-generated electron–hole pairs directly or indirectly. So, the recombination of photo-generated electron–hole pairs is suppressed, and therefore, the quantum efficiency of photocatalytic reaction is improved. This may be the possible reason for the enhancement of photocatalytic activity. The binding energy of $Sn3d_{5/2}$ (Figure 4c) was 486.36 eV, slightly lower than that of SnO_2 (>486.4 eV), might be due to oxide/oxide support interaction.

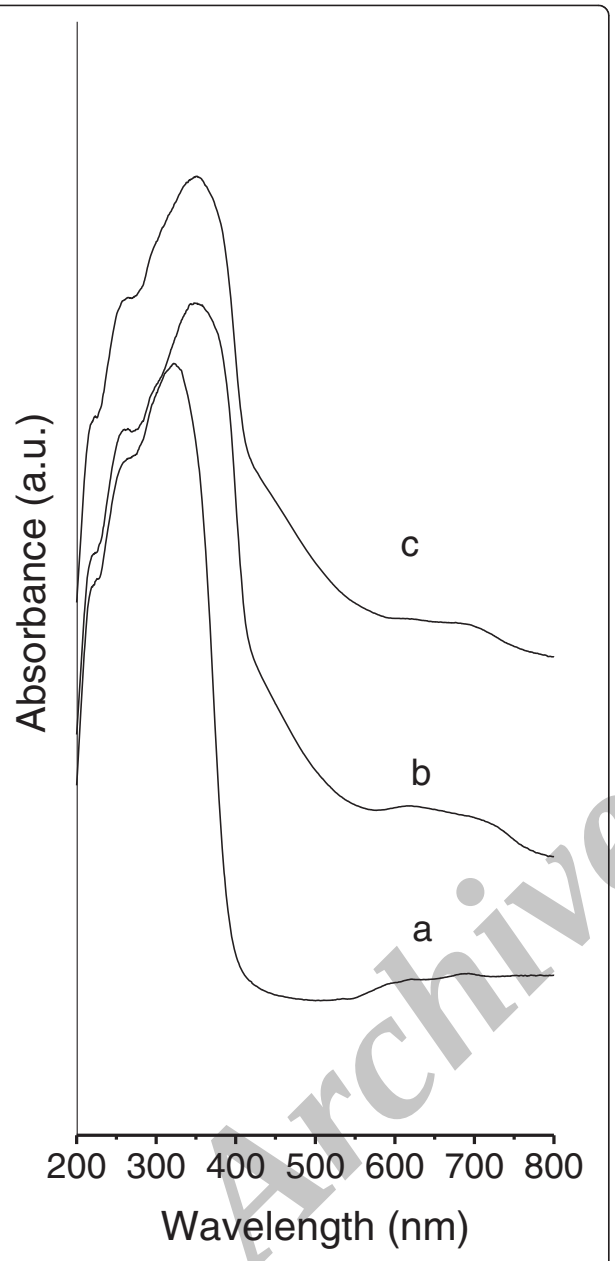

Figure 3 UV–vis DRS of the Cr_2O_3/SnO_2 photocatalyst calcined at (a) 300°C, (b) 400°C, and (c) 500°C.

Photocatalytic activity studies

The characteristic patterns of XRD, TEM, and UV–vis DRS displayed that the Cr_2O_3/SnO_2 photocatalyst calcined at 400°C for 2 h (the molar ratio of Cr to Sn is 1:2) has better crystallization, smaller crystal size, and stronger response to visible light. In order to explore the photocatalytic activity of the catalyst in the degradation of Rhodamine B solution (0.5 g/L) under visible light (λ > 400 nm), the photocatalytic behavior of the standard photocatalyst Degussa P25 was also measured as a reference. Results indicate that the Cr_2O_3/SnO_2

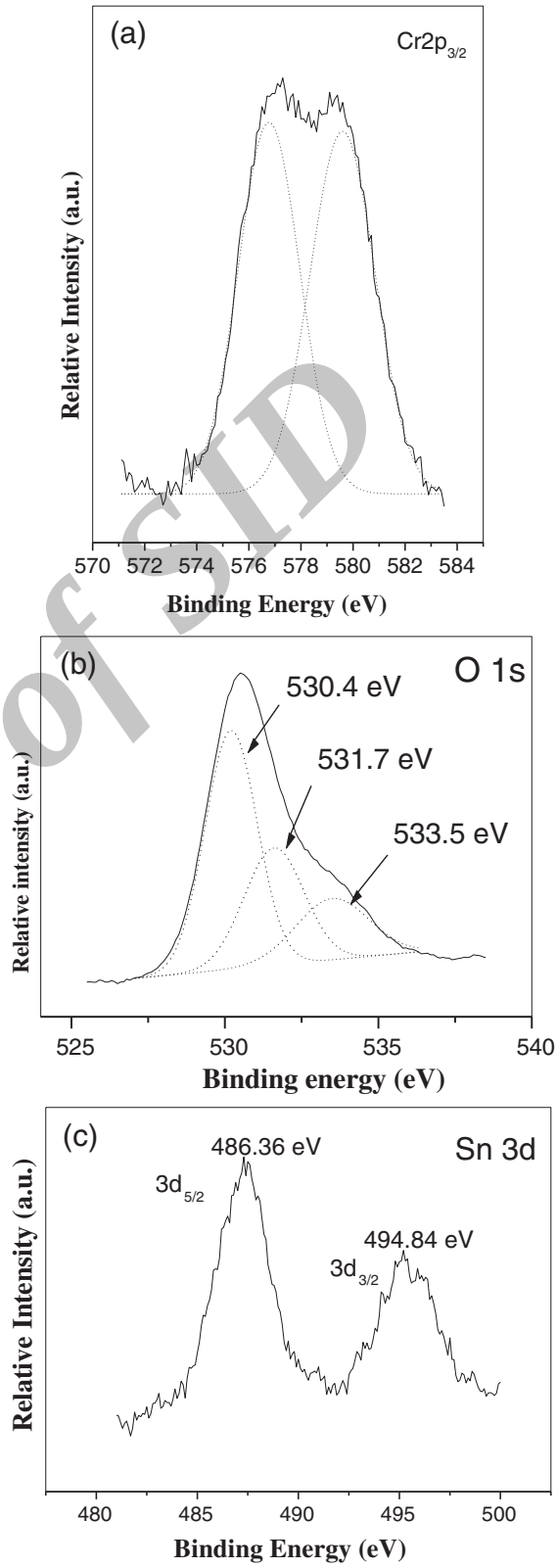

Figure 4 High-resolution XPS spectra of Cr_2O_3/SnO_2 photocatalyst calcined at 400°C for 2 h in air. (**a**) $Cr2p_{3/2}$ XPS spectra, (**b**) O 1s XPS spectra, and (**c**) Sn 3d XPS spectra.

photocatalyst displayed significantly high degradation ability for Rhodamine B, the degradation rate reached 98.0% in 60 min, which is obviously about 3.5 times higher than the value of 27.5% over Degussa P25 (Figure 5). The enhancement may be explained in terms of the synergetic effect on the specific adsorption property and efficient electron–hole separation at the Cr_2O_3/SnO_2 nanocomposite photocatalyst interfaces and surfaces. Cr_2O_3-doped SnO_2 photocatalyst have stronger reduction/oxidation capabilities, probably due to the high polymerized chromium oxide species on the catalyst surface [15]. As shown in the XPS results, formed polychromate species can substitute Ti to form a stable solid that creates a charge imbalance and must be satiated therefore; more hydroxide ions would be adsorbed on the surface to balance the charge. These hydroxide ions on the surface can accept holes generated by visible-light illumination to form hydroxyl radicals which oxidize adsorbed organic molecule.

Factors influencing the photocatalytic activity

Effect of catalyst loading

The effect of catalyst loading on the photocatalytic degradation of Rhodamine B was studied by varying the amount of Cr_2O_3/SnO_2 nanocomposite calcined at 400°C. Figure 6 showed the degradation profile of Rhodamine B with an initial concentration of 0.5 mg/L under various catalyst loadings from 0.2 to 4 g/L. It could be seen that photocatalytic degradation efficiency has increased up to 0.5 g/L and then declined with increasing catalyst loading. This could be attributed to the shadowing effect, wherein high turbidity due to high Cr_2O_3/SnO_2 nanocomposite concentration decreased the penetration depth of solar radiation. Hence, the optimal catalyst loading of 0.5 g/L was employed throughout the present study.

Effect of pH

Figure 7 presented the effect of pH value in the suspension on photocatalytic activity. The variation of pH value showed its strong influence on the Rhodamine B photodegradation. The photodegradation efficiency as a function of pH value decreased in the order of 10 > 7 > 3. It was generally accepted that the pH-dependent photodecomposition was mainly ascribed to the variation of surface charge properties of a photocatalyst. Consequently, this changed the adsorption behavior of a dye on the catalyst surface. Since Rhodamine B had a cationic configuration, its adsorption was favored in alkaline solution as demonstrated in Figure 8. The increase of pH value resulted in a higher adsorption amount of Rhodamine B on the Cr_2O_3/SnO_2 nanoparticle surface.

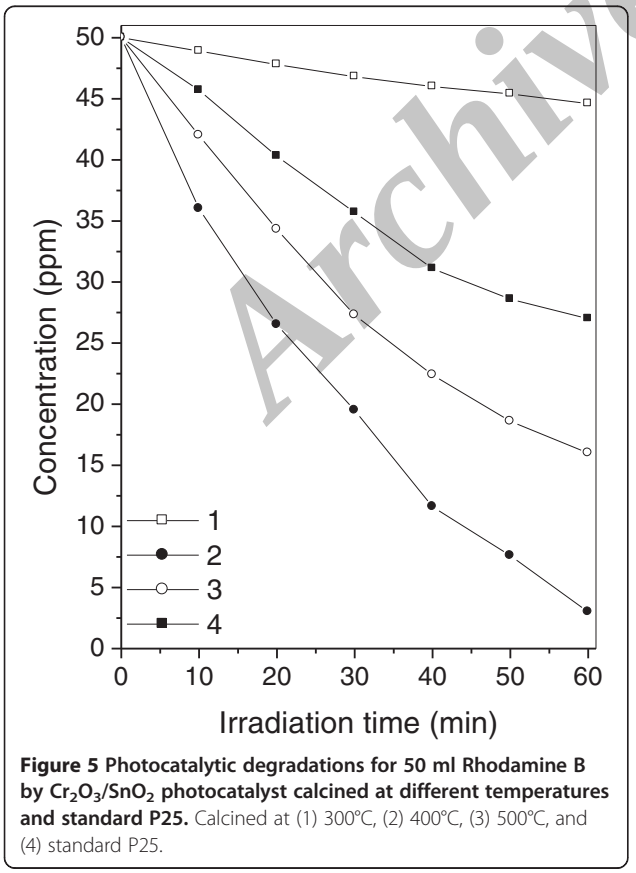

Figure 5 Photocatalytic degradations for 50 ml Rhodamine B by Cr_2O_3/SnO_2 photocatalyst calcined at different temperatures and standard P25. Calcined at (1) 300°C, (2) 400°C, (3) 500°C, and (4) standard P25.

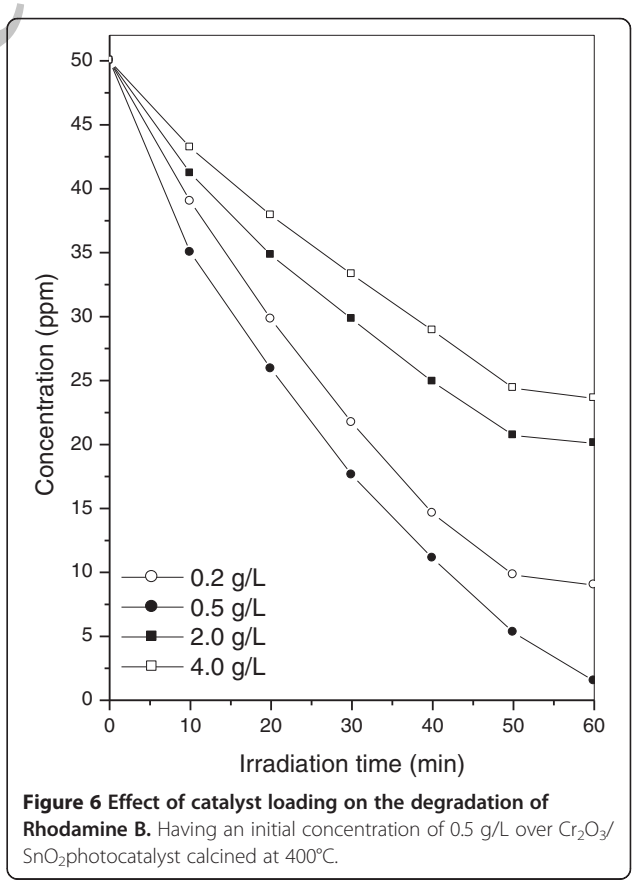

Figure 6 Effect of catalyst loading on the degradation of Rhodamine B. Having an initial concentration of 0.5 g/L over Cr_2O_3/SnO_2photocatalyst calcined at 400°C.

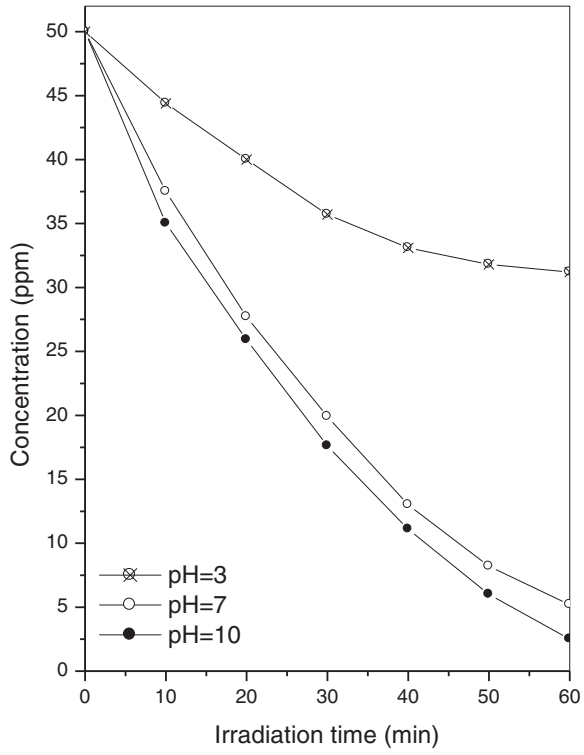

Figure 7 Effect of pH value on the degradation of Rhodamine B. Having an initial concentration of 0.5 g/L over Cr_2O_3/SnO_2 photocatalyst calcined at 400°C.

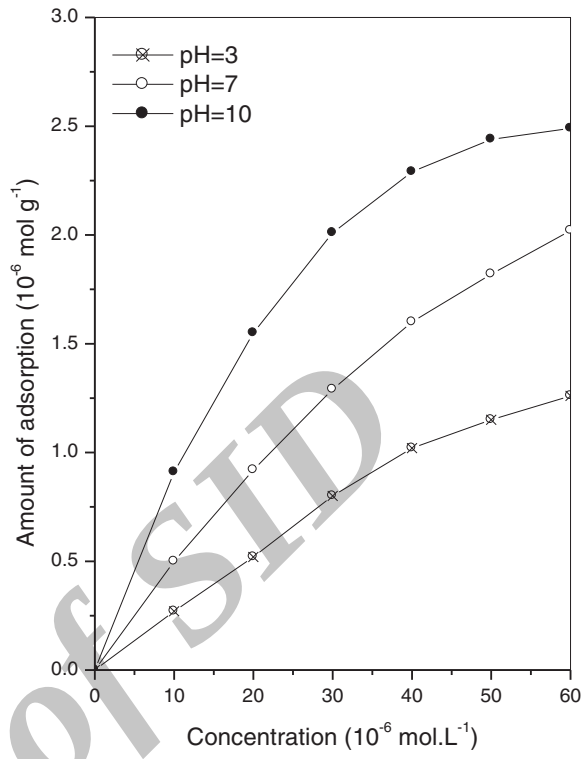

Figure 8 pH-dependent adsorption of Rhodamine B on Cr_2O_3/SnO_2 photocatalyst calcined at 400°C.

Conclusions

The novel visible-light-activated Cr_2O_3/SnO_2 nanocomposite photocatalyst was prepared by coprecipitation method. The characteristic patterns of XRD, BET, TEM, and UV–vis DRS displayed that the sample calcined at 400°C for 2 h (the molar ratio of Cr to Sn is 1:2) has better crystallization, smaller crystal size, and stronger response to visible light. The Cr_2O_3/SnO_2 photocatalyst showed remarkable photocatalytic activity compared with the standard P25 photocatalyst. Rhodamine B (98.0%) can be degraded in 60 min under illumination of the visible light ($\lambda > 400$ nm). At high catalyst loadings, penetration of the light inside the reaction medium was reduced because of the light scattering and shielding effect by catalyst particles. In addition, basic pH level of suspension was found to be beneficial for photocatalytic degradation.

Methods

Preparation of photocatalysts

The reagent grade chemicals used in preparing the samples, $CrCl_3{\cdot}6H_2O$ and $SnCl_4{\cdot}5H_2O$ were used as the starting materials. $CrCl_3{\cdot}6H_2O$ and $SnCl_4{\cdot}5H_2O$ were mixed (the molar ratio of Cr to Sn is 1:2) and dissolved in minimum amount of ethanol. The cationic surfactant cetyltrimethylammonium bromide (5%; 20 mL) in ethanol was dropped into the solution. The system was kept under constant stirring and sustaining the pH of 7 by simultaneous addition of ammonium hydroxide to form the precipitate. The precipitate was filtered and washed with deionized water until no Cl^- was found in the filtrates. Then, the wet powder was dried at about 100°C in air to form the precursor of the Cr_2O_3/SnO_2 photocatalyst. Finally, the precursors were calcined for 2 h at different temperatures in air to prepare the photocatalyst powders.

Characterization of photocatalysts

To determine the crystallite sizes and identities of the Cr_2O_3/SnO_2 nanocomposite photocatalysts, XRD analysis was carried out at room temperature using a model D8 Bruker AXS (Madison, WI, USA)with monochromatic Cu radiation (40 kV and 30 mA), over the 2θ collection range of 20° to 80°. The shapes of the samples were tested using transmission electron microscopy; FEI, Tecnai F30 HRTEM, FEG (FEI, Hillsboro, OR, USA) operated at 300 kV. The BET surface areas were determined using a Micromeritics ASAP 2010 N_2 adsorption apparatus (Norcross, GA, USA). XPS was used to study the chemical composition of the sample. The monochromatic X-ray beams of Al K_α ($h\nu$ = 1486.6 eV) and Mg K_α ($h\nu$ = 1253.6 eV) radiations were used as the excitation source. A hemispherical sector analyzer and multi channel detectors were used to detect the ejected

photoelectrons as a function of their kinetic energies. XPS spectra were recorded at pass energy of 50 eV, 5-mm slit width, and a take-off angle of 55°. The spectrometer was calibrated by determining the binding energy values of Au $4f_{7/4}$ (84.0 eV), Ag $3d_{5/2}$ (368.4 eV), and Cu $2P_{3/2}$ (932.6 eV) levels using spectrograde materials. The instrumental resolution under these conditions was 1.6 eV full-width at half-maximum for Au $4f_{7/4}$ level. The Cls (285 eV) and Au $4f_{7/4}$ (84.0 eV) were used as internal standards whenever needed.

UV–vis DRS were recorded in air at room temperature in the wavelength range of 200 to 800 nm using a PE LAMBDA35 spectrophotometer (PerkinElmer, Waltham, MA, USA).

Rhodamine B adsorption experiment

All batch equilibrium experiments were conducted in the dark. The study of Rhodamine B adsorption has been performed at room temperature. In each test, 1.5 g of Cr_2O_3/SnO_2 sample calcined at 400°C were added to 50 mL of 50 mg/L Rhodamine B solution. The equilibrium concentration was determined using centrifugation and filtration, through a Millipore filter of the suspension. The amounts of Rhodamine B adsorbed were calculated as follows:

$$n(\text{ads}) = V\Delta C$$

where n(ads) was the number of moles adsorbed; ΔC was the difference between the initial concentration, C_0 and equilibrium concentration, C_c, and V was the volume (50 mL).

Photocatalytic activity measurements

Photocatalytic degradation of Rhodamine B in aqueous solution (0.5 g/L) was carried out using a Quartz reactor under visible-light irradiation (tungsten lamp, 500 W). Air was bubbled into the solution throughout the entire experiment. A cutoff filter was placed outside the Quartz jacket to completely remove all wavelengths less than 400 nm to ensure irradiation with visible light ($\lambda > 400$ nm). About 0.5 g of photocatalyst was immersed into a 50-mL aqueous Rhodamine B. Prior to irradiation, the suspensions were magnetically stirred in the dark for 30 min to ensure establishment of an adsorption-desorption equilibrium among the photocatalyst, Rhodamine B, and atmospheric oxygen. At given irradiation time intervals, 10 mL of the suspensions are collected, and then filtered through a Millipore filter to separate the photocatalyst particles. The changes in Rhodamine B concentration were analyzed by UV-visible spectroscopy.

Competing interests

The authors declare that they have no competing interests.

Authors' contributions

RB carried out the photocatalytic degradation study, SP carried out XRD characterization of samples, BP synthesized and calcined the samples, GM carried out XPS analysis, and AG drafted the manuscript and rechecked the whole manuscript. All authors read and approved the final manuscript.

Acknowledgements

This work is financed by the University Grants Commission, New Delhi, India (Grant no. 47–2028/11).

Author details

[1]D.B.F. Dayanad College of Arts and Science, Solapur, Maharashtra 413002, India. [2]Department of Physics, Sant Gadge Baba Amravati University, Amravati, Maharashtra 444602, India. [3]Department of Chemistry, Shri Anand College of Science, Pathardi, Ahmednagar, Maharashtra 414102, India.

Received: 10 April 2013 Accepted: 24 May 2013
Published: 10 June 2013

References

1. Hoffmann, MR, Martin, ST, Choi, W, Bahnemann, DW: Environmental applications of semiconductor photocatalysis. Chem. Rev. **95**, 69–96 (1995)
2. Khan, SU, Al-shahry, M, Lngler Jr, WB: Efficient photochemical water splitting by a chemically modified n-TiO_2. Science **297**, 2243–2245 (2002)
3. Zhang, T, Oyama, T, Horikoshi, S, Zhao, J, Serpone, N, Hidaka, H: Photocatalytic decomposition of the sodium dedecylbenzene sulfonate surfactant in aqueous titania suspensions exposed to highly concentrated solar radiation and effects of additives. Appl. Catal. B: Environ. **42**, 13–24 (2003)
4. San, N, Hatipoglu, A, Kocturk, G, Cinar, Z: Photocatalytic degradation of 4-nitrophenol in aqueous TiO_2 suspensions, theoretical prediction of the intermediates. J. Photochem. Photobiol. A: Chem. **146**, 189–197 (2002)
5. Chen, S, Cao, G: Study on the photocatalytic reduction of dichromate and photocatalytic oxidation of dichlorvos. Chemosphere **60**, 1308–1315 (2005)
6. Cun, W, Jincai, Z, Xinming, W, Bixian, M, Guoying, S, Ping'an, P, Jiamo, F: Preparation, characterization and photocatalytic activity of nano-sized ZnO/SnO_2 coupled photocatalysts. Appl. Catal. B: Environ. **39**, 269–279 (2002)
7. Khan, R, Kim, TJ: Preparation and application of visible-light-responsive Ni-doped and SnO_2-coupled TiO_2 nanocomposite photocatalysts. J. Hazardous Mater. **163**, 1179–1184 (2009)
8. Guzman, C, del Angel, G, Gomez, F, Galindo-Hernandez, F, Angeles-Chavez, C: Degradation of the herbicide 2,4-dichlorophenoxyacetic acid over Au/TiO_2-CeO_2 photocatalysts: effect of the CeO_2 content on the photoactivity. Catal. Today **166**, 146–151 (2011)
9. Kanai, N, Nuida, T, Ueta, K, Hashimoto, K, Watanabe, T, Ohsaki, H: Photocatalytic efficiency of TiO_2/SnO_2 thin film stacks prepared by DC magnetron sputtering. Vaccum **74**, 723–727 (2004)
10. Wang, C, Shi, H, Li, Y: Synthesis and characterization of natural zeolite supported Cr-doped TiO_2 photocatalysts. Appl. Surf. Sci. **258**, 4328–4333 (2012)
11. Hamadanian, M, Jabbari, V, Gravand, A: Dependence of energy conversion efficiency of dye-sensitized solar cells on the annealing temperature of TiO_2 nanoparticles. Mater. Sci. Semicond. Process. **15**, 371–379 (2012)
12. Weckhuysen, B, Wachs, I, Schoonheydt, R: Surface chemistry and spectroscopy of chromium in inorganic oxides. Chem. Rev. **96**, 3327–3350 (1996)
13. Radecka, M, Zakrzewska, K, Wierzbicka, M, Gorzkowska, A, Komornicki, S: Study of the TiO_2-Cr_2O_3 system for photoelectrolytic decomposition of water. Solid State Ion. **157**, 379–386 (2003)
14. Yim, SD: Nam, I–S: Characteristics of chromium oxides supported on TiO_2 and Al_2O_3 for the decomposition of perchloroethylene. J. Catal. **221**, 601–611 (2004)
15. Hakuli, A, Harlin, ME, Backman, LB, Krause, AOI: Dehydrogenation of *i*-butane on Cr_2O_3/SiO_2 catalysts. J. Catal. **184**, 349–356 (1999)

doi:10.1186/2193-8865-3-46
Cite this article as: Bhosale *et al.*: Visible-light-activated nanocomposite photocatalyst of Cr_2O_3/SnO_2. *Journal Of Nanostructure in Chemistry* 2013 3:46.